CORE

Metadata, citation and similar papers at core.ac.uk

Provided by Nottingham ePrints

MOLECULAR CRYSTALS AND LIQUID CRYSTALS [Template]

Effect of dicationic ionic liquids on lyotropic liquid crystals formed by a binary system composed of Triton-X 100 and water

Leila T. Thieghi[a], Luiz S. Longo Jr.[a,b], Peter Licence [b], Sarah Alves[a]

[a] Instituto de Ciências Ambientais, Químicas e Farmacêuticas, Universidade Federal de São Paulo, Diadema - SP, Brazil

[b] The GlaxoSmithKline Carbon Neutral Laboratory, School of Chemistry, The University of Nottingham, Nottingham NG7 2RD, United Kingdom

ABSTRACT

In this work, binary mixtures of a non-ionic surfactant (Triton X-100) and water were studied with concentrations of 30%wt H_2O, showing, lamellar mesophase at temperatures below 10ºC. Different dicationic ionic liquids were used for doping these mesophases: 1,n-bis(3-methylimidazolium-1-yl)alkane, 1,n-bis(1-methylpyrrolidinium-1-yl)alkane and 1,n-bis(pyridinium-N-yl)alkane dibromide, where n = 6 and 8. Polarized Optical Microscopy and Small-Angle X-ray Scattering were used for identifying the mesophases and the influence of different dicationic ionic liquids on the lyotropic liquid crystals phase transitions. The addition of dicationic ionic liquids to the lyotropic liquid crystals samples led to changes in transition temperature and in mesophase structure itself (such as characteristic distances).

ARTICLE HISTORY

Received dd Month yyyy

Accepted dd Month yyyy

KEYWORDS

lyotropic liquid crystal; dicationic ionic liquids; binary system Triton-X; lamellar mesophase

CONTACT

Leila Thomazelli Thieghi • leila.thieghi@unifesp.br • Rua Prof. Artur Riedel, n° 275 - Jd. Eldorado - CEP: 09972-270 - Diadema – SP, Brazil

Introduction

Triton-X 100/water binary system has a well-known phase diagram[1] in which the main ordered phase is hexagonal, and also have a small region of lamellar phase at low temperature (from 0ºC to 6ºC) and high concentrations (from 65 to 80wt% of Triton X-100).

Ionic liquids (ILs) are salts with low melting points (< 100º C), solely composed of mobile ions. They are often referred to as designer materials due to the infinite possibility of combinations for anions and cations, thus rendering ionic liquids with their own set of physical or chemical properties, suitable for specific applications in several fields, such as electrochemistry[2], catalysis[3,4,5,6,7], CO_2 absorption[8] and gas chromatography stationary phases[9], among others.

Ionic liquid crystals are a class of liquid-crystalline compounds that contain ionic units in the mesophase. Due to the presence of anions and cations, ionic liquid crystals are ion conductive, enabling the construction of materials with anisotropic electric current conductivity[10]. In general, ionic interactions tend to stabilise lamellar mesophases, due to an ion-ion stacking and electrostatic interactions[11].

Exploration of the lyotropic liquid crystals (LLC) behaviours of surfactants in ionic liquids may provide a better understanding of intermolecular actions in self-assembly and also improve some properties of LLC, like better thermostability compared to those constructed in aqueous media. In these systems, various LLC phases could be detected, including the normal hexagonal, lamellar, sponge and reverse bicontinuous cubic phases, some of them not detected in aqueous media. The modification of the alkyl chain length in surfactant was reported as a possible way to come from a reversal to a normal mesophase[12].

The introduction of self-assembled nanostructures into IL systems is an efficient way to enhance their molecular recognition ability which favours the development of high-performance separation technologies, advanced sensors, drug-delivery systems, and materials synthesis[13].

In this work, LLC in lamellar mesophases doped with dicationic ionic liquids (DIL) were investigated under Small Angle X-ray Scattering (SAXS) and Polarized Optical Microscopy (POM) techniques. The DIL's used are geminal dicationic liquids formed of imidazolium, pyrrolidinium, and pyridinium-based cations containing Br^- as an anion (Figure 1). Two different linkage chains were studied (n = 6 and n = 8), and the effects of these structural variations on the mesophases were examined.

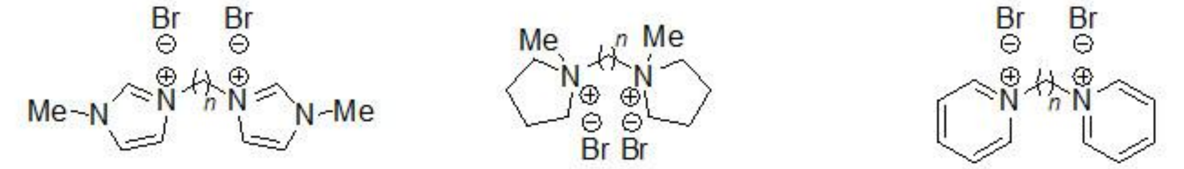

$[C_6(C_1Im)_2][Br_2]$ *n* = 6 **DIL-1**
$[C_8(C_1Im)_2][Br_2]$ *n* = 8 **DIL-2**
$[C_6(C_1Pyrr)_2][Br_2]$ *n* = 6 **DIL-3**
$[C_8(C_1Pyrr)_2][Br_2]$ *n* = 8 **DIL-4**
$[C_6(Py)_2][Br_2]$ *n* = 6 **DIL-5**

Figure 1. Dicationic dibromide ionic liquids **DIL-1-5** used in this study.

Experimental Section

Materials

Lyotropic Liquid Crystals

Binary mixtures of a non-ionic surfactant and water were prepared with Triton X-100 from Sigma Aldrich and distilled water. The concentration of 70%wt %Triton X-100 was used for lamellar mesophase[14]. *Samples were prepared* by mixing all components in a vortex and using an ultrasound bath and centrifugation for homogenization. For doped LLC, solid DIL-**1-5** were directlly added to the lamellar matrix.

Dicationic Ionic Liquids

All germinal dibromide dicationic ionic liquids were prepared in high purity using standard methods described in the literature[15-22]. The **DIL-1-5** compounds were obtained as pure amorphous white solids in 60-85% yield, and were fully characterized by ^{1}H and ^{13}C NMR.

1,6-Bis(1-methylimidazolium-3-yl)hexane dibromide $[C_6(C_1Im)_2][Br_2]$ (DIL-1)[15,16]**.** ^{1}H NMR (300 MHz, D_2O) δ 1.26-1.39 (m, 4H), 1.76-1.92 (m, 4H), 3.87 (s, 6H), 4.17 (t, *J* = 7.1 Hz, 4H), 7.41 (s, 2H), 7.45 (s, 2H), 8.69 (s, 2H); ^{13}C NMR (75 MHz, D_2O) δ 24.8, 29.1, 35.7, 49.4, 122.2, 123.5, 135.8.

1,8-Bis(1-methylimidazolium-3-yl)octane dibromide $[C_8(C_1Im)_2][Br_2]$ (DIL-2) [15,17]**.** ^{1}H NMR (300 MHz, D_2O) δ 1.30 (br s, 8H), 1.77-1.89 (m, 4H), 3.87 (s, 6H), 4.17 (t, *J* = 7.1 Hz, 4H), 7.41 (s, 2H), 7.46 (s, 2H), 8.70 (s, 2H); ^{13}C NMR (100 MHz, D_2O) δ 25.2, 27.8, 29.1, 35.7, 49.5, 122.2, 123.5, 135.8.

1,6-Bis(1-methylpyrrolidium-3-yl)hexane dibromide $[C_6(C_1Pyrr)_2][Br_2]$ (DIL-3) [18],[19]. ^{1}H NMR (300 MHz, D_2O) δ 1.38-1.49 (m, 4H), 1.74-1.89 (m, 4H), 2.11-2.26 (m, 8H), 3.03 (s, 6H), 3.30-3.36 (m, 4H), 3.42-3.57 (m, 8H); ^{13}C NMR (75 MHz, D_2O) δ 21.3, 23.0, 25.3, 48.1, 64.0, 64.3.

1,8-Bis(1-methylpyrrolidium-3-yl)octane dibromide $[C_8(C_1Pyrr)_2][Br_2]$ (DIL-4) [20],[21] **.** ^{1}H NMR (300 MHz, D_2O) δ 1.3-1.42 (m, 8H), 1.71-1.83 (m, 4H), 2.12-2.25 (m, 8H), 3.02 (s, 6H), 3.28-3.33 (m, 4H), 3.42-3.52 (m, 8H); ^{13}C NMR (75 MHz, D_2O) δ 21.3, 23.0, 25.2, 27.9, 48.0, 64.3.

1,6-Bis(pyridinium-1-yl)hexane dibromide [$C_6(Py)_2$][Br_2] (DIL-5)[22] **.** ^{1}H NMR (300 MHz, D_2O) δ 1.35-1.45 (m, 4H), 1.96-2.09 (m, 4H), 4.61 (t, *J* = 7.4 Hz, 4H), 8.06 (t, J = 7.1 Hz, 4H), 8.50-8,57 (m, 2H), 8.84 (d, J = 5.7 Hz, 4H). ^{13}C NMR (75 MHz, D_2O) δ 24.8, 30.3, 61.7, 128.3, 144.2, 145.6.

Polarized Optical Microscopy

The samples were encapsulated inside micro slides 0.2 mm thickness sealed with Parafilm®, placed in an INSTEC HS1-i hot stage system, and positioned in a Leitz orthoplan-pol microscope. Micrographics were taken with a digital camera coupled to the microscope and temperature was variated from 6°C to 40°C, to avoid sample evaporation.

Small Angle X-ray Scattering

SAXS experiments were performed in a Xenocs Xeuss SAXS/WAXS system. It has a GeniX beam delivery system with a Cu anode X-ray tube (λ = 0.15411 nm), two scatterless slits as a collimator, and a two-dimensional Dectris Pilatus 300 K detector which registers the patterns. The beam delivered to the samples has a square cross-section of 0.5 mm × 0.5 mm. The exposure time for SAXS measurements in each sample was 15 min. The circular averaging of the two-dimensional images were made using the SOLEIL Foxtrot software. The scattering vector modulus is defined as $q = (4\pi \sin\theta)/\lambda$, where 2θ is the scattering angle. Samples were encapsulated in capillary glass tubes 1.5mm diameter and measurements were performed at a controlled temperature of 6°C.

Results and discussion

Firstly, all prepared samples were observed in a polarised optical microscope positioned on a hot stage, as described before. The temperature was variated from about 6^{o}C up to 40^{o}C, and micrographics were taken with a digital camera coupled to the microscope; In Figure 2 showed some of them.

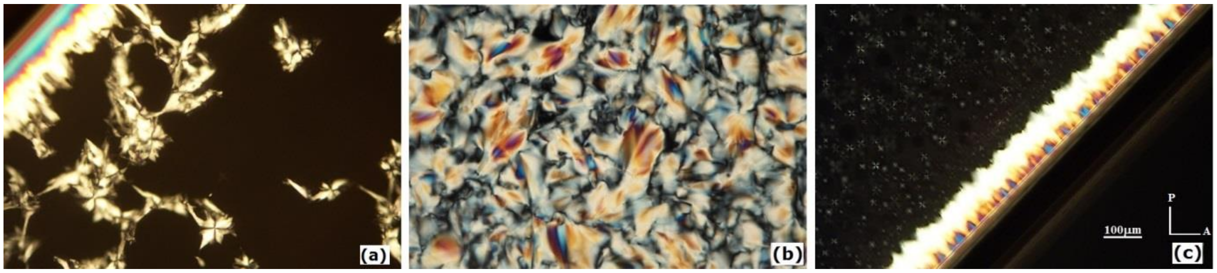

Figure 2. Microscopic textures of the 70 wt% Triton-X100-water binary system; The samples were observed for temperatures from 6^{o}C to 40^{o}C, at a rate of about 5 °C/min, encapsulated in micro slide de 0.2 mm thickness using with 10X magnification, at 45^{o} with a polariser (P) and analyser (A). (a) lamellar matrix doped with DIL-5, exhibiting lamellar texture at 9^{o}C, (b) lamellar matrix doped with DIL-2 exhibiting lamellar texture at 5.3^{o}C, (c) non-doped lamellar matrix, exhibiting Maltese crosses in the centre and colourful borders at 9^{o}C.

POM enabled the construction of a phase diagram, Figure 3, with transitions temperatures for all investigated samples. Phase transitions temperatures slightly change: for DIL's with n = 8; a small decreasing of transition temperature lamellar-isotropic phase was noticed; for DIL's with n = 6 a small region (about 2^{o}C) of coexistence phase appeared between lamellar and isotropic phase, reducing the lamellar phase in comparison to n = 8.

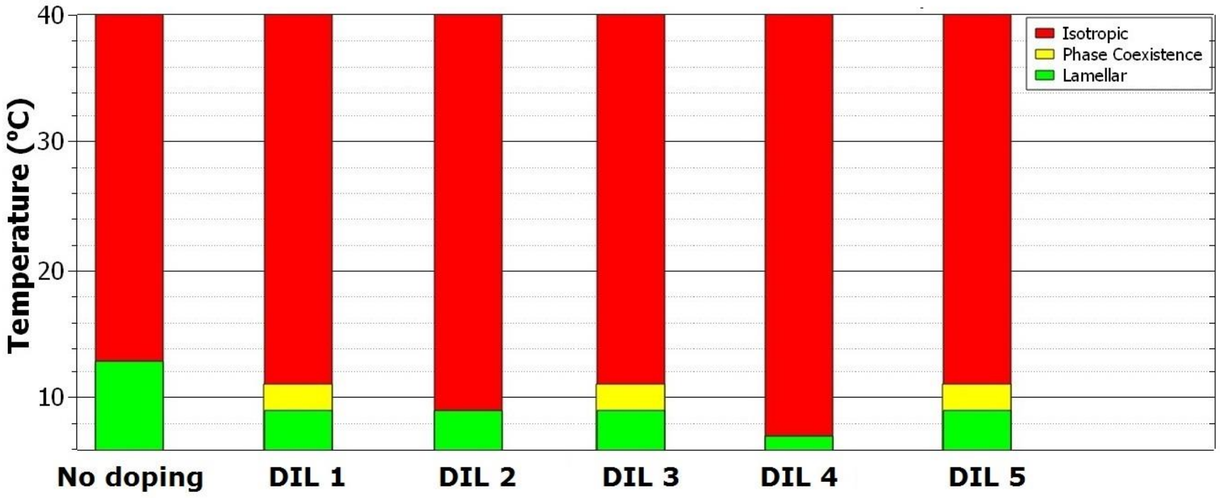

Figure 3. Phase Transitions Temperature for all samples.

SAXS experiments were performed at 6°C of temperature, in lamellar mesophase, for all samples. Figure 4 shows SAXS results for the lamellar matrix (black line) and samples doped with three different DIL: DIL-1 (marine line), DIL-3 (olive line) and DIL-5. All curves presented the lamellar mesophase signature, a relation 1:2 of the Bragg peaks positions[23],[24]. The addition of the dicationic ionic liquids increased the intensity of SAXS curves in 50% up to 100%, pointing to more ordered structures. In detail, it is also possible to see a peak position deviation for small values of scattering vector, q, for first and second order peaks, that means an enlargement of the lamellar structure for all DILs. The values for lamellar periodicity[23] (spacing), $d=2\pi/q_1$, where q_1 refers to the first peak, and DIL's concentrations for each sample can be found in Table 1.

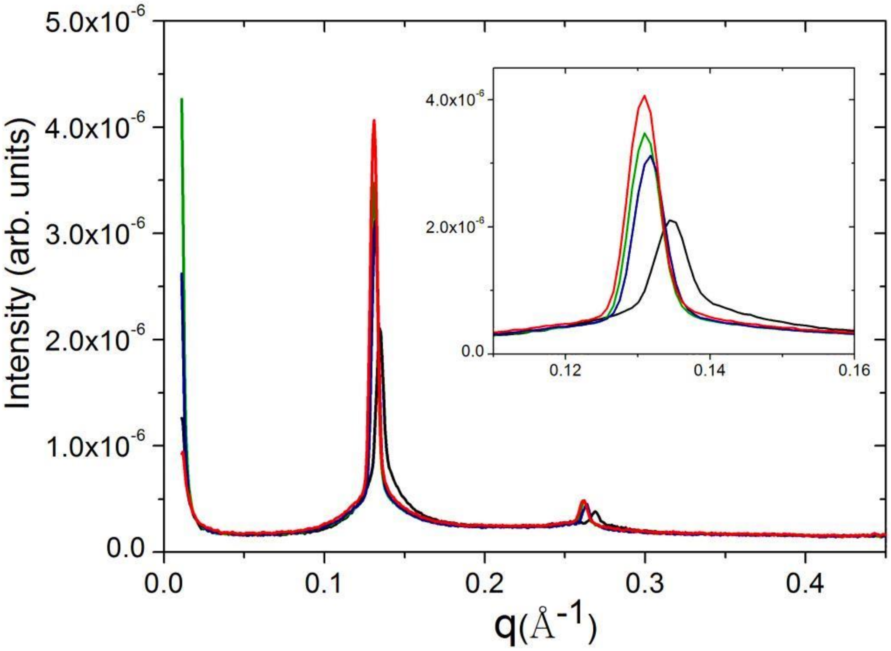

Figure 4 SAXS results for lamellar matrix and three samples doped with different DIL with six carbons (n=6) in the central chain. Lamellar matrix (black line) and samples doped with DIL-5 (red line), DIL-1 (marine line) and DIL-3 (olive line).The error bars are comparable to the line thickness and were omitted for clarity.

Table 1. Results of lamellar periodicity for lamellar phase obtained from SAXS experiments at 6°C.

Abbreviation	Dicationic ionic liquid dopant	DIL concentration (mols%)	Bragg peak positions relationship	d (Å)
L	No doping	0	1:2	46.61
DIL-1	$C_6(C_1Im)_2(Br)_2$	0.22	1:2	47.67
DIL-2	$C_8(C_1Im)_2(Br)_2$	0.28	1:2	47.38
DIL-3	$C_6(C_1Pyrr)_2(Br)_2$	0.40	1:2	48.00
DIL-4	$C_8(C_1Pyrr)_2(Br)_2$	0.22	1:2	47.42
DIL-5	$C_6(Py)_2(Br)_2$	0.48	1:2	48.00

A comparison of the influence of the number of carbons (n = 6 and n = 8) in the central chain of DIL was done (Figure 5) for $C_n(C_1Im)_2Br_2$ and $C_n(C_1Pyrr)_2Br_2$. There is a small shift to the right of peak positions with increasing carbon number, but the relation 1:2 is preserved, as well the peak intensity, indicating that lamellar mesophase is preserved but with a small lamellar periodicity *d*.

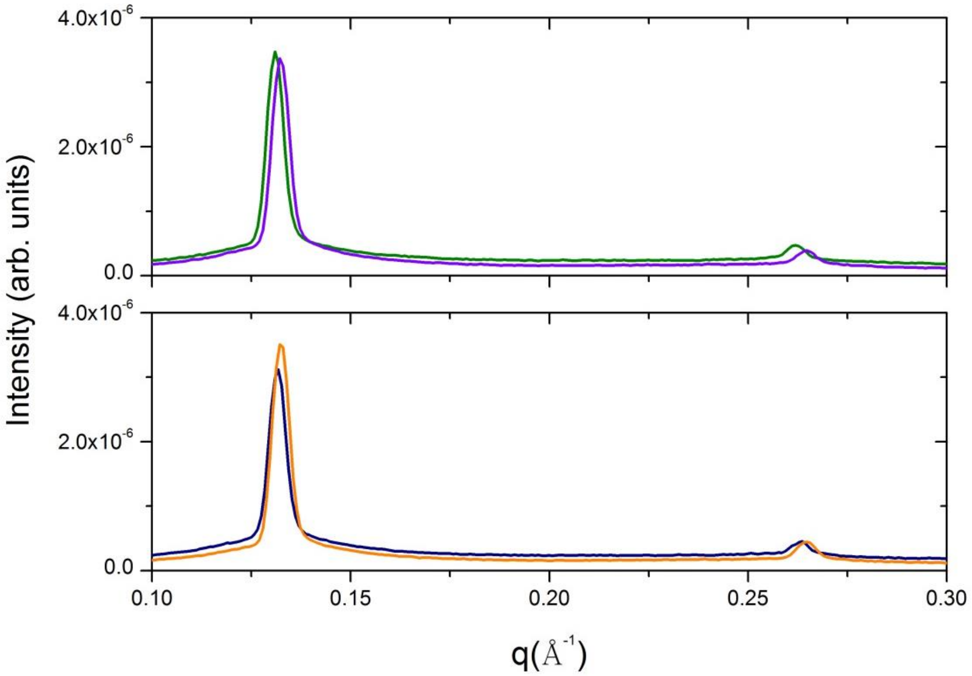

Figure 5 SAXS results for $C_n(C_1Im)_2Br_2$ (above) and $C_n(C_1Pyrr)_2Br_2$ (below) for n=6 and n=8. DIL-1 (olive line), DIL-2 (purple line), DIL-3 (marine line) and DIL-4 (orange line). The error bars are comparable to the line thickness and were omitted for clarity.

Using the lamellar periodicity, *d*, which was found for the pure lamellar mesophase, we calculated membranes thickness, d_m, and water layer thickness, d_w, where $d = d_m+d_w$, and $d = d_m/(1-vf_w)$, vf_w is the volumetric water fraction, getting d_m=31.97 Å and d_w=14.64 Å. The addition of the DIL's studied in this paper in a lamellar mesophase lead to a more ordered lamellar mesophase, with a larger lamellar periodicity *d*. The increasing in lamellar periodicity with DIL doping may be due to an increase of water layer thickness or membrane thickness.

Table 2. Water Layer thickness, d_w, for lamellar phase obtained from SAXS experiments at 6°C.

Abbreviation	d_w(Å)
L	14.64
DIL-1	16.04
DIL-2	15.64
DIL-3	16.09
DIL-4	15.46
DIL-5	16.22

DILs molecules are shorter than Triton-X molecules, and its interaction with the hydrophilic part of Triton-X promote an enlargement of the water layer, more significant for DIL-3 and DIL-5, in comparison with DIL-1 (Table 2).

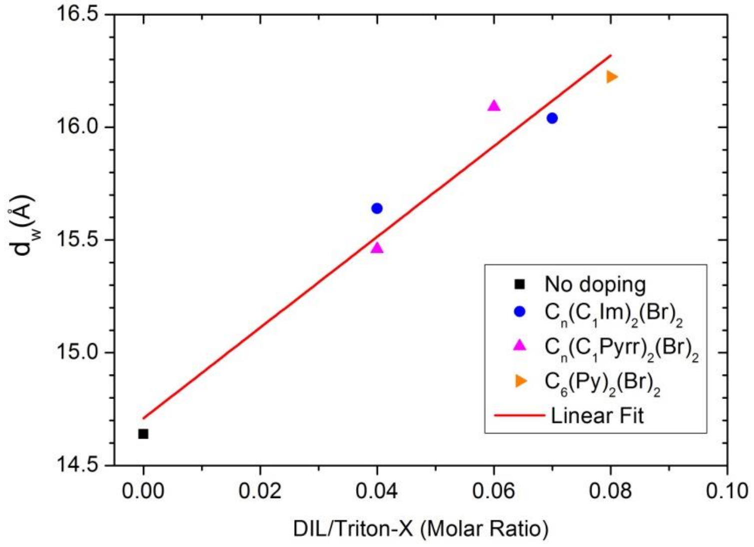

Figure 6: Water Layer thickness, d_w, as a function of DIL/Triton-X molar ratio.

Figure 6 shows the dependence of water layer thickness (d_w) with the proportion of the number of DIL molecules compared with Triton X (DIL/TRX). The increase of DIL/TRX causes an increase of d_w. For DILs with $n = 6$, the values of DIL/TRX are 0.08, 0.07 and 0.06, for DIL-5, DIL-1 and DIL-3, respectively, while for DILs with $n = 8$ are 0.04 for DIL-2 and 0.03 for DIL-4. This result shows that the lamellar periodicity mainly depends on of the molar ratio between DIL and Triton-X. Molecular interactions between Triton-X and DIL may be contributing to a tight molecular arrangement, leading to a more rigid structure.

When comparing changes as a function of alkyl chain length (n = 6 or 8) it is possible to verify that DILs with smaller chain (n = 6) promote an increasing in lamellar periodicity larger than that promoted with DILs with larger chain (n = 8).

As a conclusion, the doping LLC with DIL practically does not affect phase transition temperatures and promote a better organisation of the system. The periodicity of the lamellar phase can be tunable with DIL dopings, what can be very useful to applications for lamellar LLC.

Acknowledgments

Authors are thankful to INCT-Fluidos Complexos for SAXS and POM facilities.

Disclosures

The authors have no relevant financial or nonfinancial relationships to the products or services described, reviewed, evaluated or compared in this presentation.

Funding

This work was supported by São Paulo Research Foundation (FAPESP), Coordination for the Improvement of Higher Education Personnel (CAPES), and National Council for Scientific and Technological Development (CNPq).

References

1 Beyer, K., *Journal of Colloid and Interface Science*, **1982**, 86(1), 73-89.
2 Ohno, H., *Ed. Electrochemical Aspects of Ionic Liquids*, 2nd ed.; Wiley: NJ, 2011.
3 Welton, T. *Chem. Rev.*, **1999**, 99, 2071-2084.
4 Dupont, J.; de Souza, R. F.; Suarez, P. A. Z. *Chem. Rev*,. **2002**, 102, 3667-3692.
5 Pârvulescu, V. I.; Hardacre, C. *Chem. Rev.*, **2007**, 107, 2615-2665.
6 Hallett, J. P.; Welton, T. *Chem. Rev.*, **2011**, 111, 3508-3576.
7 Zhang, Q.; Zhang, S.; Deng, Y. *Green Chem.*, **2011**, 13, 2619-2637.

8 Pinto, A. M.; Rodriguez, H.; Colon, Y. J.; Arce, A., Jr.; Arce, A.; Soto, A. *Ind. Eng. Chem. Res.*, **2013**, 52, 5975-5985.

9 Baltazar, Q. Q.; Leininger, S. K.; Anderson, J. L.; *J. Chromatogr. A*, **2008**, 1182, 119-127.

10 Axenov, K.V., Laschat, S., *Materials* **2011**, *4*, 206-259

11 Binnemans, K., *Chem. Rev.*, **2005**, 105, 4148-4204.

12 LI QinTang & CHEN Xiao, *Chinese Science Bulletin*, **2017**, 62, 478-485,

13 Xianxian Liu,Qiwei Yang,Zongbi Bao,Baogen Su,Zhiguo Zhang,Qilong Ren,Yiwen Yang,and Huabin Xing, *Chem.Eur.J.*, **2015**,21,9150–9156

14 Figueiredo Neto, A.M.; Salinas, S.R.A.; *The Physics of Lyotropic Liquid Crystals*, Oxford U.P., IF-USP, SP, 2005.

15 Shirota,H., Mandai,T., Fukazawa,H., Kato, T., *J. Chem. Eng. Data*, **2011**, 56, 2453–2459.

16 Anderson,J.L., Ding,R., Ellern,A., Armstrong,D.W., *J. AM. CHEM. SOC.*, **2005**, 127, 593-604.

17 Chen,F., Yang,X.,Wu,Z., Han,B., *J. Org. Chem*., **2016**, 81, 9494−9498.

18 Wong,W., Ho,K., Lee,L.Y.S., Lam,K., Zhou,Z., Chan,T.H., Wong,K., *ACS Catal*., **2011**, 1, 116–119

19 Almeida,R.K.S., Gómez-Hortigüela,L., Pinar,A.B., Peréz-Pariente,J.,*Microporous and Mesoporous Materials*, **2016,** 232, 218-226

20 Huang,D., Bai,X., Zheng,L., *J. Phys. Chem. C*, **2011**, 115, 14641–14647

21 Ding,G., Zhang,W., Zhang,Z., Guo,D., Tang,G., Li,Y., Li,J., Cao,Y., *Anal Bioanal Chem.*, **2017**, 409, 4581-4592

22 Zahn,T.J., Weinbaum,C., Gibbs,R.A., *Bioorganic & Medicinal Chemistry Letters*, **2010**, 20, 1763–1766

23 Alexandridis, P., Olsson,U., Lindman, B., *Langmuir* **1998**, 14(10), 2627-2638.

24 S.T. Hyde, *Identification of lyotropic liquid crystalline mesophases, Chap. 16 of Handbook of Applied Surface and Colloid Chemistry*, K. Holmberg, ed., J. Wiley & Sons, 2001 330.